# Systemic Magnetic Targeting of Pure-Antiestrogen-Loaded Superparamagnetic Nanovesicles for Effective Therapy of Hormone-Dependent Breast Cancers

Vincent Plassat, Jack-Michel Renoir, Gwennhael Autret, Véronique Marsaud, Christine Ménager, Olivier Clément, Sylviane Lesieur

Journal of Bioanalysis & Biomedicine

Plassat et al., J Bioanal Biomed 2013, 5:2
DOI: 10.4172/1948-593X.1000077

Research Article Open Access

# Systemic Magnetic Targeting of Pure-Antiestrogen-Loaded Superparamagnetic Nanovesicles for Effective Therapy of Hormone-Dependent Breast Cancers

**Vincent Plassat[1], Jack-Michel Renoir[1], Gwennhael Autret[2], Véronique Marsaud[1], Christine Ménager[3], Olivier Clément[2] and Sylviane Lesieur[1]***

[1]*Laboratoire Physico-Chimie des Systèmes Polyphasés, UMR CNRS 8612, Université Paris-Sud 11, F-92296 Châtenay-Malabry, France*
[2]*Laboratoire de Recherche en Imagerie, INSERM U494, Faculté de Médecine Necker Enfants Malades, F-75014 Paris, France*
[3]*Laboratoire des Liquides Ioniques et Interfaces Chargés, UMR CNRS 7612, Université Pierre et Marie Curie, F-75252 Paris cedex, France*

## Abstract

Systemic hormone therapy of breast cancer often suffers from severe side effects mainly due to non-specific drug delivery. To overcome this limitation, we propose an effective strategy based on the association of the selective estrogen receptor down-regulator RU-58668 (RU) that acts as a pure hormone antagonist, with magnetic-fluid-loaded liposomes (MFLs) which can be driven selectively into the tumors by a magnetic field gradient. MFLs consisted in 200-nm unilamellar phospholipid vesicles entrapping superparamagnetic iron oxide nanocrystals, fluorescently labeled and coated by poly(ethylene glycol) (PEG) chains ensuring long plasmatic half-life. Significant antitumoral activity of antiestrogen at doses usually sub-therapeutic was demonstrated against MCF-7 tumors xenografts in nude mice after weekly intravenous administration of RU-loaded MFLs followed by 4-hour exposure to an external 0.44-T magnet (155 T/m magnetic field gradient). The magnetic accumulation of RU-MFLs at the origin of improved antitumor activity was checked *in vivo* by MRI using the magnetic fluid as intrinsic contrast agent, fibered confocal fluorescence microscopy to track the lipid vesicle structures, *ex-vivo* tumor histology by confocal fluorescence microscopy or iron oxide staining, and KI-67 immunostaining to reveal RU anti-proliferative activity. Our findings establish that magnetic targeting results in significant therapeutic benefit by highly concentrating RU-loaded liposomes in the tumor tissue according to amplified EPR effect and significantly enhanced drug delivery at the intracellular level. The use of superparamagnetic liposomes to target magnetically estrogen antagonists offers a reliable direction to treat hormone-dependent breast tumors with possible combination of MRI diagnosis.

**Abbreviations:** EPC: Egg-yolk-extracted L-αPhosphatidylCholine; $DSPE\text{-}PEG_{2000}$: 1, 2-diacyl-SN-glycero-3-phosphoethanolamine-N-[methoxy(poly(ethylene glycol))-2000]; Rho-PE: N-(lissamine rhodamine B sulfonyl) phosphatidylethanolamine;RU 58668 (RU): 11-[4-[5-[(4,4,5,5,5,-pentafluoropentyl)sulfonyl]pentyloxy]phenyl]-estra-1,3,5(10)-triene-3,17β-diol (657 $g.mol^{-1}$)

## Introduction

Breast cancer is the most prevalent cancer among women and one of the main leading causes of death each year [1]. Local treatments, consisting of surgery and radiotherapy, usually deserve to be combined with systemic adjuvant treatments to impede malignant cell growing and reduce the risks of recurrence and metastasis [2]. The treatment of invasive breast cancer very often calls for hormone therapy since growth, survival and differentiation of most of mammary tumor cells are determined by estrogen binding to its receptor transcription factors [3]. Medicines currently prescribed either decrease the hormone rate like aromatase inhibitors [4] or act as antagonists by blocking the estrogen-receptors as exemplified by tamoxifen [5,6]. Despite its effectiveness for the treatment of estrogen-sensitive breast cancers, conventional hormone therapy can have deleterious side effects such as bone thinning [7], risk of osteoporosis and developing endometrial cancer [8] or resistance [9]. A strategy to overcome such complications is to enhance drug therapeutic index by increasing their concentration in the malignant cells while decreasing the exposure in normal host tissues. This can be achieved by using long-circulating nanocarriers which have opened new therapeutic approaches exploiting the so-called "enhanced permeability and retention (EPR) effect". The dysregulated nature of tumor angiogenesis indeed causes vasculature hyperpermeability [10] allowing submicronic particulate systems like stealth liposomes consisting of lipid vesicles sterically stabilized by poly(ethylene glycol) (PEG) to extravasate from the abnormal vessels and accumulate in tumor tissue [11,12]. PEG-ylated liposomes have relative biological inertia, weak immunogenicity and low intrinsic toxicity justifying clinical use [13].

However, EPR effect does not totally spare the healthy tissues and progress in active targeting of active substances is required to improve the performance of stealth liposomes. The best advanced method lies in a biochemical approach that consists of attaching onto the liposome surface mainly antibodies, integrin-specific ligands or folate residues [14,15]. In this work, we propose an alternative and promising direction based on the use of a magnetic force to guide and accumulate in tumors drug-loaded superparamagnetic nanovesicles mainly composed of phospholipids. If this strategy has been experienced for non-lipid systems [16-18], comparatively fewer studies have been focused on magnetic liposomes [19]. In this work, we implemented preclinical

***Corresponding author:** Sylviane Lesieur, Laboratoire Physico-Chimie des Systèmes Polyphasés, UMR CNRS 8612, 5 rue J.B. Clément, F-92296 Châtenay-Malabry, France; E-mail: sylviane.lesieur@u-psud.fr

**Received** November 01, 2011; **Accepted** November 08, 2011; **Published** November 12, 2011

**Citation:** Plassat V, Renoir JM, Autret G, Marsaud V, Ménager C, et al. (2013) Systemic Magnetic Targeting of Pure-Antiestrogen-Loaded Superparamagnetic Nanovesicles for Effective Therapy of Hormone-Dependent Breast Cancers. J Bioanal Biomed 5: 028-035. doi:10.4172/1948-593X.1000077

experiments to show *in vivo* the efficacy of magnetic targeting for systemic therapy of hormone-dependent breast cancer tumors. The magnetic-fluid-loaded liposomes (MFLs) specially used here were fluorescently labelled by a rhodamine-based lipid marker and exhibited superparamagentic behaviour suitable for magnetic guidance and magnetic resonance imaging (MRI) [20-26]. The selective estrogen receptor down-regulator RU 58668 (RU) was stably incorporated within the vesicle bilayer. RU efficiently binds to estrogen-receptor alpha (ERα), inducing its fast delocalization and rapid 26S-proteasome-mediated degradation in the nucleus of breast-cancer cells [27]. Moreover it limits endometrial carcinogenesis [28,29] and interestingly ranks among the alternative drugs to treat invasive estrogen-sensitive breast-cancers in the case of tamoxifen-resistance [30-32]. MFLs result from the encapsulation of maghemite nanocrystals into 200-nm PEG-ylated phosphatidylcholine vesicles with plasmatic half-life of 12.5 h [24]. Very recently, we have demonstrated *in-vitro* efficacy of magnetic targeting of RU-loaded MFLs to treat human breast-cancer MCF-7 cells [33]. The purpose here focused on a preclinical study on human MCF-7 tumor xenografts in mice and targeted delivery of intravenously administered RU-loaded MFLs by applying a magnetic field gradient of 155 T/m produced by a small 0.44-T magnet externally placed onto the tumors. Tumor growth monitoring, *in-vivo* imaging and deep histological analyzes were implemented to provide insight into the biological fate of RU-MFLs. The ultimate aim was to highlight the therapeutic potency of drug magnetic targeting by intentionnaly administering sub-therapeutic doses of the estrogen antagonist to mice bearing tumor xenografts moreover exposed to unfavorable hormone-hyperstimulation.

## Materials and Methods

### Chemicals

Chloroform solutions of egg-yolk-extracted L-α-phosphatidylcholine (EPC), 1,2-diacyl-SN-glycero-3-phosphoethanolamine-N-[methoxy(poly(ethylene glycol))-2000] (DSPE-$PEG_{2000}$) and N-(lissamine rhodamine B sulfonyl) phosphatidylethanolamine (Rho-PE) were purchased from Avanti Polar Lipids (Alabaster, AL). Sodium chloride, sodium citrate, *N*-[2-hydroxyethyl]piperazine-*N*'-[2-ethanesulfonic acid] (HEPES) and pH 6,2 Tris–EDTA (10mM citric acid, 2mM EDTA, 0.05% v/v Tween 20) were provided by Sigma (Saint-Quentin Fallavier, France), 1X phosphate buffered saline aqueous solution (1X PBS) by Gibco/Invitrogen (Cergy Pontoise, France). The buffer used was 108mM NaCl, 20 mM sodium citrate, 10mM HEPES, pH 7.4 and 285 mOsm. Compound 11β-[4-[5-[(4,4,5,5,5,-pentafluoropentyl)sulfonyl]pentyloxy]phenyl]-estra-1,3,5(10)-triene-3,17β-diol (657 $g.mol^{-1}$) or RU 58668 (RU) was a gift from P. Van de Velde (Hoechst Marion Roussel, Romainville, France).

### Animals

All animal experiments were performed on female nude mice at least 7 weeks old (Janvier, Le Genest Saint Isle, France). The experiments were carried out in compliance with the recommendations of the European Economic Community (86/609/EEC) and the French National Committee (decree 86/848) for the care and use of laboratory animals. The mice were housed in metabolism cages at 22°C-controlled temperature. Sterilized food (AO4C-10, SAFE, Augy, France) and water were given *ad libitum* and 12-h light cycles were respected. Otherwise stated, anaesthesia were performed by injecting mice intramuscularly with a 120µL mixture containing 24.7 µL of Imalgene 500® (Mérial, Lyon, France), 7.7 µL of Valium® 10mg/mL (Roche, France), 12.4 µL of atropine 0.1% (Laboratoire Renaudin, Itxassou, France) and 75.2 µL of sterilized water.

### Magnetic-fluid-loaded liposome preparation

Nanocrystals of maghemite ($\gamma$-$Fe_2O_3$) stabilized by coating with citrate anions were adjusted in concentration (4.8 M Fe(III) by flame spectroscopy) by ultrafiltration through a 50-kD MACROSEP filter (Fisher Scientific Labosi, France) followed by addition of the buffer used for liposome preparation [20,34,35].Rhodamine-labeled magnetic-fluid-loaded liposomes (MFLs) were prepared by hydration of a thin lipid film (EPC:DSPE-$PEG_{2000}$:Rho-PE; 94:5:1 mol%) by adding equal volumes of maghemite particles suspension and buffer to get 19.9 ± 0.7 mM total lipid concentration (checked by enzymatic assay, Phospholipides Enzymatiques PAP 150, Biomérieux, France) before sequential extrusion through polycarbonate filters with 0.8 µm/0.4 µm/0.2 µm decreasing pore diameters (PORETICS, Osmotics, Livermore, USA) [22-25]. RU containing MFLs (RU-MFLs) were similarly obtained from a mixed film of drug and lipids by removing under nitrogen stream the solvents from a mixed solution in chloroform/ethanol (50:50 vol/vol) at the desired RU to lipids ratio before 12-hour lyophilization [33]. Non-entrapped maghemite particles were removed by gel exclusion chromatography with the buffer as eluent and a 0.4 cm × 5.8 cm Sephacryl S1000 superfine (Pharmacia) microcolumn (TERUMO 1 mL-syringe). Final Fe(III) concentrations of 28 ± 1.4 mM and 31.0 ± 1.6 mM (checked by flame spectroscopy) were found for MFLs and RU-MFLs preparations, respectively.

Drug loading (3.75 ± 0.05 moles of antiestrogen per 100 moles of total lipids) was controlled by UV absorbance at 232 nm (Lambda 2 double-beam spectrophotometer, Perkin-Elmer) after RU extraction from liposomes by butan-1-ol (Carlo Erba Reagenti, France). Briefly, 900 µL of butan-1-ol were added to 100 µL of the initial liposome sample before vigorous stirring by vortex followed by 3-min centrifugation (3000 g). The UV absorbance of the clear supernatant was recorded after dilution in butan-1-ol (1:10, v/v) and RU concentration calculated from a standard curve in butanol/buffer (1:100, v/v) solution.

Size analysis was performed by using a photon correlator spectrometer (10 mW HeNe 632.8-nm laser, Zetasizer Nano ZS90, Malvern Instruments). Hydrodynamic diameter values $d_h$ were calculated from the measured translational diffusion coefficients D of the particles according to the Stokes-Einstein law for non-interacting spherical particles: $d_h = k_B T/3\pi\eta D$ ($k_B$, Boltzman constant; η, dispersant viscosity). Unimodal distribution analysis in triplicate indicated 4-month stable hydrodynamic diameters of 17 ± 5 nm (maghemite particles), 192 ± 52 nm (MFLs) and 212 ± 47 nm (RU-MFLs).

### Tumor xenograft experiments

Original tumors were generated by percutaneous injection of tumor cells in four female nude mice before being transplanted into new animals [36]. Estrogen-sensitive human breast adenocarcinoma MCF-7 cells (ATCC, Molsheim France) were cultured in Dulbecco's modified Eagle's medium (DMEM BioWhittaker, Cambrex Bio Science Verviers, Belgium) supplemented with L-glutamine (2 mM), penicillin (50 IU/mL), streptomycin (50 IU/mL), 10% fetal calf serum (FCS) and maintained at 37°C and 5% $CO_2$ in humidified atmosphere. Under these conditions, the cell number increased by a factor 2 ± 0.5

during a 30-hour incubation period. Sub-confluent MCF-7 cells were resuspended in the culture medium (5-10×$10^7$ cells/mol) and mixed with equal volume of Matrigel® (BD Bioscience, Le Pont de Claix, France). The final cell suspension was percutaneously injected into the left flank of 7-8 weeks aged female nude mice then treated twice weekly with 50 µg of 17β-Estradiol (Sigma) in ethanolic solution by skin deposition. The injected cells were grown as tumors for 5 to 7 weeks until reaching around 250 $mm^3$ in median volume estimated as equal to 0.5x(width$^2$)x(length). Then the mice were sacrificed by cervical rupture under anaesthesia and biopsies (1.5 ± 0.5 $mm^3$) were taken from two selected tumors (237 and 295 $mm^3$, respectively) and transplanted under the skin on the lower left of the back in new mice for treatment experiments. Fragments from the same tumor were used for a given animal group and allowed to grow for 6 to 8 weeks before treatment.

### Tumor treatment experiments

Five groups of six mice (7 weeks old) were studied. Three control groups received either no treatment or 200-µL injections of drug-free MFLs (4 µmoles total lipids, 5.6 µmoles iron oxide per injection) or 100-µL injections of RU in glucose 5% (0.15 µmoles RU per injection). The two other groups received 200-µL injections of RU-MFLs (0.15 µmoles RU, 4 µmoles total lipids, 6.2 µmoles iron oxide per injection). One of these groups was exposed for 4 hours after each injection to 155 T/m magnetic field gradient produced by a 0.44 T cylindrical magnet (6 mm diameter, 6 mm height, 1.25 g) externally fixed onto the location of the tumor by an adhesive band (Elastoplasm, BSN Medical, Le Mans, France). Tumors were stimulated twice weekly with 50 µg of estradiol in ethanolic solution deposited on mice skin at the tumor level [36,37]. All injections were performed into the retro-orbital venous sinus [37-39] under anaesthesia one day per week for seven consecutive weeks. The animals were monitored and weighed daily. No death occurred and no significant loss of weight could be noticed all along the experiment period. Tumor median volumes (0.5x(width$^2$)x(length)) were regularly measured by using an electronic digital caliper.

At the end of the experiments, the mice were sacrificed under anaesthesia by cervical rupture. Tumors and uterus were carefully removed and weighed. Halves of tumors were placed in 4% paraformaldehyde (v/v in 1X PBS, pH 7.4, 25°C) for 4 days, rinsed with and stored in 1X PBS at 4°C. Buffer was changed once after 24-hour storage and again 24 hours before specimen preparation for histology. The other halves were fixed in FineFix® (Milestone medical, Sorisole, Italy) and stored in the dark at 4°C.

### In-vivo magnetic resonance imaging (MRI)

All images were acquired with a 1.5-T Achieva clinical MR scanner (Philips, Eindhoven, The Netherlands) using a custom-built 3-cm-diameter Helmholtz coil for signal transmission and reception. After being anesthetized with isoflurane-oxygen (2%-98%), the animals were placed in the coil where anesthesia was maintained. T2-weighted gradient-echo (SPGR T2, 365/10–25, 30° flip angle) and three-dimensional (3D) spoiled gradient-echo (SPGR 3D, 37.5/8.6, 30° flip angle) pulse sequences were performed with 4 x 4-cm field of view (FOV) and 256x128 matrix, one acquired signal and 2-mm (SPGR sequences), 1.5-mm (T2 gradient-echo) section thickness.

### In-vivo fibered confocal fluorescence microscopy

The fibered confocal fluorescence microscope (CFM) device (Cell-Vizio® system, Mauna Kea Technologies, Paris, France), was equipped with a laser scanner unit functioning at 488 nm (LSU-488), a flexible fibered microprobe (ProFlex S-5.0, 1.5 mm diameter, 15 µm axial resolution, 5 µm lateral resolution, 500×600 µm field of view, 500-650 nm bandwith collection) and ImageCell® processing software (Image Cell 3.5.4, Mauna Kea Technologies, Paris, France). For visualization *in vivo in situ*, mice were anesthetized by intraperitoneal injection of 0.1 mL/10g of a 4:1 vol/vol mixture of xylazine 2% (16 mg/kg, Rompum, Bayer, Leverkusen, Germany) and ketamine 500 (100 mg/kg, Imalgene, Rhône Mérieux, Lyon, France) and surgically prepared: 1-centimeter long buttonhole slit was performed through the skin at the tumor level. The probe was maintained in contact with the surface of the tumor which was regularly hydrated by a saline buffer (physiological serum, Gibco/Invitrogen, Cergy Pontoise, France). Image of total vasculature was recorded by injecting 100 µL of 20 mg/mL FITC-dextran (5.$10^5$ g/mol, Sigma) just before microscopy.

### Ex-vivo confocal fluorescence microscopy

Organ extracts were put in 8-mL poly(ethylene) boxes filled with OCT (optimum cutting temperature, Compound Gurr®, BDH, England) and plunged into liquid nitrogen for 2 minutes. Freeze tissue blocks were cut in a cryomicrotome (CM 3050S, Leica, Germany) at -21°C into 18-20 µm thick sections. Confocal fluorescence microscopy was performed with a CLSM 510 microscope (Zeiss, Germany) coupled with a LSM 5 Image Browser (Zeiss) and an air-cooled ion laser providing excitation light at 488 nm and 543 nm. Slowfade®, (Molecular Probes, USA) was used to ensure fluorescence protection. Images were obtained by using Plan Apochromat 14x and 20x objective lens (Zeiss) and 505-550 and 563-659 nm emission filters. The selected pictures were representative of a number of images from 6 sections per mouse taken from 3 distinct animals per group.

### Iron oxide staining and visualization by optical microscopy

Tumor FineFix® specimens were dehydrated by successive immersions in toluene (Carlo Erba Reagenti, France) and ethanol (Carlo Erba Reagenti), before embedding in paraffin (Paraplast®, Tyco Healthcare group LP, Mansfield, MA, USA). Paraffin blocks were cut into 5-µm thick sections (Leica 2035 microtome, Leica Inst. GmbH, Nussloch, Germany). Paraffin was removed by rinsing in toluene and in ethanol followed by rehydration in 1X PBS. Perls blue staining was performed by a 15-min incubation at 20°C in 2% w/v potassium ferrocyanide (Sigma) solubilized in freshly prepared 2% v/v hydrochloric acid, before washing in 1X PBS. The sections were then stained with 2.5 g/L eosine (Réactif RAL, Martillac, France) and 10g/L saffron (Réactif RAL, Martillac, France) solutions, washed in 1X PBS and mounted with Eukitt® medium (Sigma).

Slices were examined with a λ/4 retarded-in-white light by using a NIKON E600 Eclipse direct microscope (Champigny/Marne, France) equipped with a long focus objective (LWD40x 0.55; 0-2 mm). Micrographs were recorded at 20°C with a color NIKON Coolpix 950 camera (1600x1200 pixels resolution). The selected pictures were representative of a number of images from 6 sections per mouse taken from 3 distinct animals per group.

### Immunohistochemical experiments

Tumor slices were prepared as for iron oxide staining. Heat-induced epitope retrieval was carried out with pH 6,2 Tris–EDTA at 90°C for 7 minutes, left at 20°C for 10 minutes and washed with 1X

PBS. Endogenous peroxidase activity was quenched through 30-min reaction with 3% $H_2O_2$ (Sigma) in 1X PBS. The slices were washed with 1X PBS, placed in cover plates (Shandon, Detroit, MI, USA) and incubated in blocking serum (Vectastain Elite ABC, Vector Laboratories, Burlingame, CA, USA) for 10 minutes before 30-minute contact with Ki-67 antibodies (1:100 concentration, clone MIB-1, M 7240, DakoCytomation, Glostrup, Denmark). Immunostaining was performed with Vectastain Elite ABC kit (Vector Laboratories) and diaminobenzidine as chromogen (Sigma). Cell chromatin and nucleoli were stained with Mayer's hemalum (Réactif RAL, Martillac, France). All slides (mounted with Eukitt® medium, Sigma) were immunostained in cover plates the same day, guaranteeing a perfectly standardized intensity of staining, both for the immunohistochemical signal and for the counterstaining. The selected pictures were representative of a number of images from 6 sections per mouse taken from 3 distinct animals per group.

## Results

### Antitumor activity

Intravenous treatment of nude mice bearing subcutaneous MCF-7 tumor xenografts with magnetic-fluid-loaded liposomes incorporating RU (RU-MFLs) obviously retained the growing ability of the tumors with noticeably much greater efficiency under the influence of an external magnet (Figure 1, 2). Contrarywise, drug-free magnetoliposomes led to a significant increase in median tumor volume very close to that observed for the non-treated mice. It is worth noting that highly proliferative state of the tumor cells was intentionally maintained all along the experiments by 17β-estradiol application twice weekly. In these conditions, injections of the free drug solution only slightly slowed down tumor growth, thereby highlighting the real gain of antitumor activity provided by the combination of liposomal formulation of RU and magnet apposition. Compared to free RU solution, the relative volume of the tumors xenografted in mice treated with RU-MFLs without magnet was reduced by a factor 1.36 ($p<0.001$) against a factor up to 1.82 ($p<0.001$) in the presence of magnetic field gradient (Figure 2). For each group of animals, no significant increase in the uterus weights was noticed, showing the anti-uterotrophic activity of the antiestrogen whatever its formulation.

### In vivo evidence of magnetic targeting

The fate of injected RU-MFLs was followed by magnetic resonance imaging (MRI), especially sensitive to the iron oxide nanocrystals inside the liposomes which indeed act as efficient T2 contrast agents. Mice treated with RU-MFLs during seven weeks were examined 4 hours after the seventh and last injection and compared to mice of the untreated group. The MR images well confirmed the difference in size of the tumors as a function of the applied treatment (. 3). Tumors treated by drug-loaded liposomes clearly showed negative contrast enhancement using T2-weighted gradient-echo sequences revealing concentrated magnetic fluid [21]. Injection without magnet led solely to vascular detection whereas the tumor tissue exposed to the magnetic field gradient appeared markedly darker not only in the vessels but also over a wider area of the tumor tissue, precisely at the inner periphery where the magnet was placed (Figure 3). This demonstrates the efficacy of magnetic force to concentrate intact RU-loaded magnetoliposomes into tumors since maghemite nanoparticles injected alone present very short plasmatic half-life and cannot be guided *in vivo* by the same kind of external magnet as that used here [21,22,24].

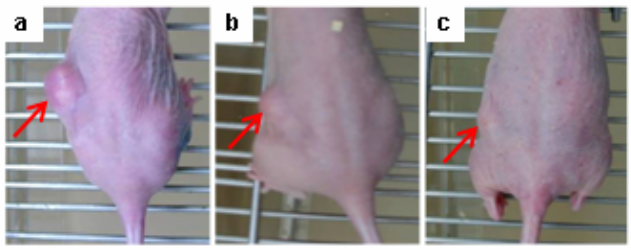


**Figure 1: Mice bearing subcutaneous MCF-7 tumor xenografts (arrows) at seven-week growth.** Mice without treatment (a) or weekly treated with RU-MFLs (4.3mg/week/kg) without (b) or with 4-hour magnet apposition (c).

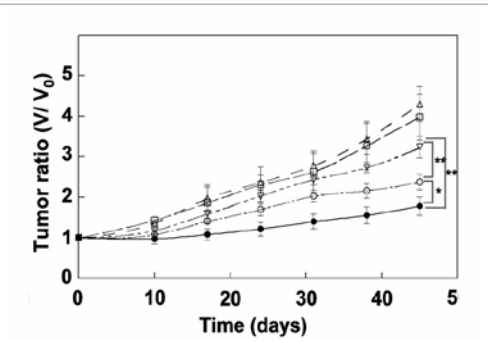


**Figure 2: MCF-7 tumor xenografts evolution versus time**. Five groups of mice were studied: the first group was not treated (△), the second one was weekly injected with drug-free MFLs (□), the last three other groups were weekly treated (4.3mg RU/week/kg), either in glucose 5% solution (▽) or incorporated within MFLs with (●) or without (○) a 0.44-T external magnet (155 T/m magnetic field gradient) placed onto the tumor for 4 hours after injection. Tumor growth was reported by the ratio of average median volume (V) measured for each animal group on week n (n=1-7) to that measured on week 0 ($V_0$); symbols * and **mean $p<0.01$ and $p<0.001$, respectively.

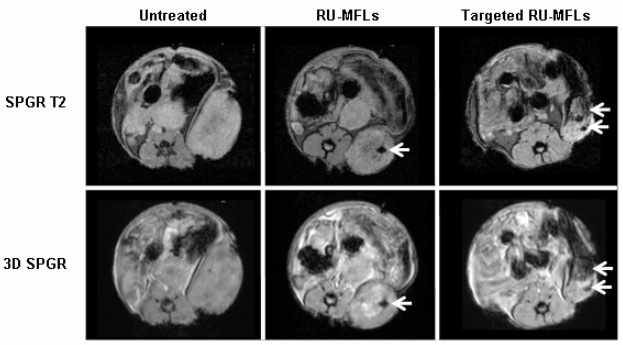


**Figure 3: *In-vivo* MRI.** The MR images were obtained from either untreated mice (left column) or weekly injected ones by RU-MFLs (4.3mg/week/kg) without (middle column) or in the presence of a 0.44-T magnet (155 T/m magnetic field gradient) placed onto the tumor (targeted RU-MFLs, right column). Arrows show negative contrast enhancement due to high iron oxide concentration.

*In-vivo* fibered confocal fluorescence spectroscopy allowed to show whether rhodamine fluorescence signal that should reveal the lipid vesicle structures could be actually observed in the peripheral vascular network or not. First, Images in Figure 4a from an untreated mouse injected with FITC-dextran exhibited rather rich vascularisation of

the tumor indeed propitious to intravenous drug delivery. In the case of tumor xenografts from RU-MFL-treated mice 4 hours after their seventh injection without magnet, only few sparse thodamine signals could be seen (data not shown). In contrast, images recorded after magnet-exposure revealed clusters of strong rhodamine fluorescence intensity moving along the circulatory pathway (Figure 4b-d). Taking into account that the magnet was removed before imaging, the mobility of the vesicle structures showed that the significant intratumoral accumulation of in-blood persistent liposomes in vascular level by magnetic guidance was reversible.

## Intratumoral pathway and antiproliferative efficacy

Histological analysis of tumor sections after seven-week treatment with RU-MFLs clearly showed rhodamine-labeled fluorescent liposomes in more or less extended areas inside vessels. However, whereas these fluorescent clusters were hardly distinguished in tumors not submitted to magnetic field gradient (Figure 5a), they appeared significantly more numerous and of higher intensity in the magnet-exposed tumors (Figure 5b). For these last only, extravascular localization was also found as exemplified by the intense and spread

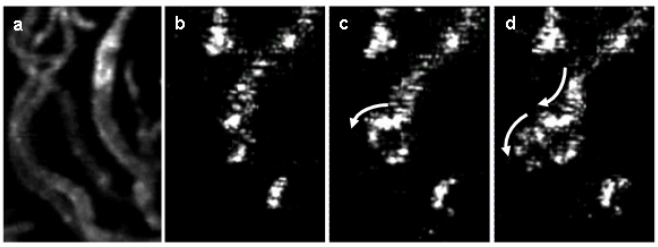


**Figure 4: *In-vivo* fibered confocal fluorescence microscopy**. The optical probe was placed on the surface of the MCF-7 xenografted tumors by means of a minimal skin incision which preserved the integrity of the tissue. Control tumor immediately after FITC-dextran injection $5.10^5$ g/mol (100 µL of 20 mg/mL solution) of an untreated mouse (a). Typical time-resolved viewing of tumors carried by mice treated weekly with Rho-PE labelled RU-MFLs (4.3mg/week/kg) 4 hours after the seventh injection and exposition to a 0.44 T magnet (155 T/m magnetic field gradient) (b-d). Images b to d show rhodamine signal due to the injected liposomes as obtained every two seconds and 10 min after magnet removal. Arrows indicate circulating RU-MFLs.

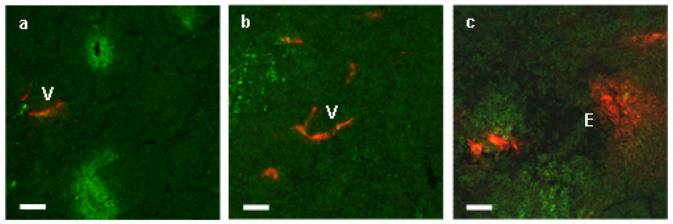


**Figure 5: Histological analysis of tumor slices by confocal fluorescence microscopy.** The tumors were taken from mice injected weekly by RU-MFLs (0.15 µmoles RU (4.3mg/week/kg) either without (a) or in the presence of a 0.44-T magnet (155 T/m magnetic field gradient) placed at the tumor location (b, c). The tumors were removed 18 hours after the seventh injection. Intrinsic fluorescence of the tumoral tissue was visualized in green by laser-beam excitation wavelength at 488 nm (emission recording in the 505-550 nm range) while Rho-PE fluorescence labeling MFLs, in red on the images, were distinctly revealed by laser-beam excitation wavelength at 543 nm (emission recording in the 563-659 nm range). Control tumor slices from an untreated animal led to no fluorescence emission at 543 nm excitation. Areas resulted from the projection of twenty 20µm-thick images (magnification x 20). Note the presence of rhodamine fluorescence characteristic of liposome structures inside the blood vessels (V) and in the extravascular region of the targeted tumor (E). White bars represent 50 µm.

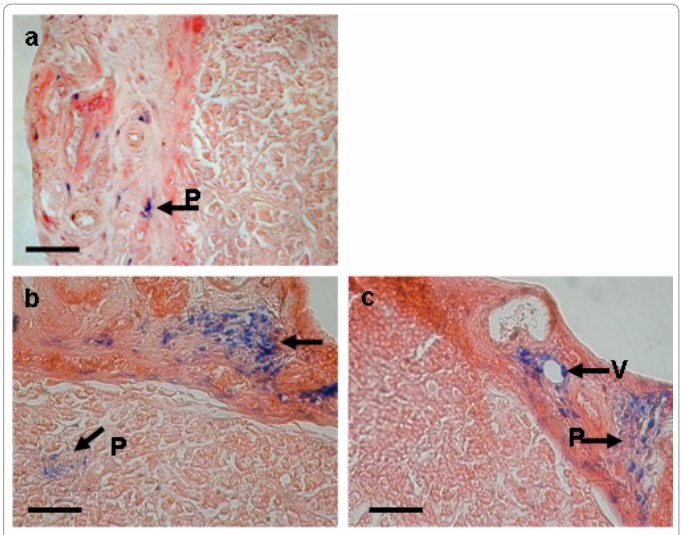


**Figure 6: Histological analysis of tumor slices by optical microscopy after iron oxide staining**. The tumors were taken from mice injected weekly by RU-MFLs (0.15 µmoles RU (4.3mg/week/kg) either without (a) or in the presence of a 0.44-T magnet (155 T/m magnetic field gradient) placed at the tumor location (b,c). The sections were stained with eosine/saffron for cell visualization and 2% w/v potassium ferrocyanide in acid medium (perls blue solution) for iron detection. Note the presence of iron oxide characteristic of liposome content viewed inside the blood vessels (V) and in the parenchyma (P). Black bars represent 50 µm.

signal seen in (Figure 5c). These observations ascertain the efficiency of magnetic targeting to accumulate the lipid vesicles within the tumor, from intraluminal blood compartment towards extravascular surrounding tissue. The intratumor pathway of the lipid vesicles coincided with that of iron oxide. Blue coloration revealing iron oxide was indeed rare in the non-targeted tumors (Figure 6a) whereas the magnet-exposed tumors displayed numerous blue inclusions, mainly found in the richly vascularised rim but also within the central region (Figures 6b,c).

For untreated and drug-free MFLs injected mice, tumor cells present strong KI-67 antigen staining (Figures 7a, b). The proportion of black core remained high upon free RU solution administration whereas it was significantly decreased by treatment with RU-MFLs and totally vanished when magnetic field gradient was applied (Figures 7c-e). The quantitative evolution of KI-67 index as a function of treatment makes clear that magnetic targeting produces greater anti-proliferative activity of the antiestrogen which could only be due to better intracellular delivery (Figure 7f).

## Discussion

MCF-7 cell line ranks among the prominent models for investigation of estrogen receptor-positive breast cancer and easily responses to estradiol stimulation by markedly increased proliferation rates while being particularly sensitive to down-regulation by antagonistic action of antiestrogens [37]. In this respect, the steroid antagonist RU displays *in vitro* highly anti-proliferative activity and induces *in vivo* long-term regression of MCF-7 tumors implanted in nude mice at an effective dose of 50 mg/kg/week [31]. In contrast, at a dose as low as that administered in the present study (4.3 mg/kg/week), only stationary state of the tumor xenografts could be achieved, moreover providing that moderate hormone stimulation was used, typically 250 µg/kg

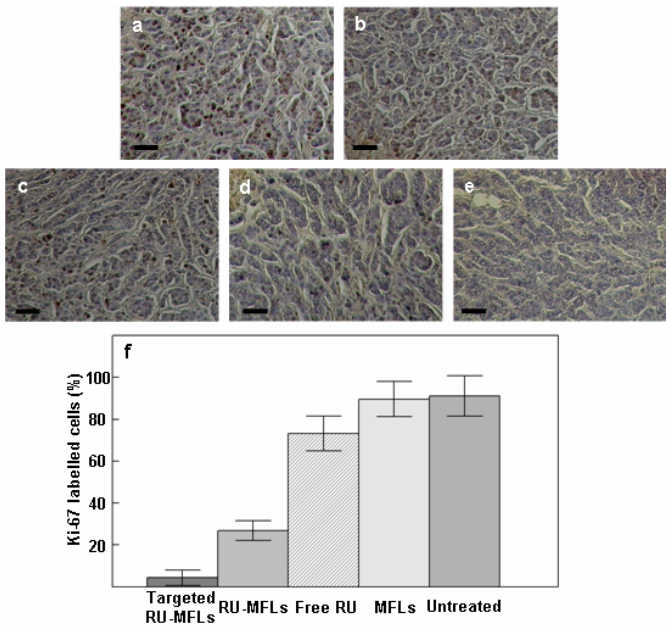


**Figure 7: Evaluation of antiproliferative activity.** Optical micrographs correspond to tumor slices from mice allocated to untreated group (a), group weekly injected with drug-free MFLs (b, MFLs) and groups weekly treated through intravenous administrations of 0.15 µmoles RU (4,3mg/week/kg) in glucose 5% solution (c) or via RU-MFLs without (d) or with (e) 4-hour application of as 0.44-T magnet (155 T/m magnetic field gradient). Sections were stained with Mayer's hemalum after KI-67 antigen diaminobenzidine-detection. Histogram reports on the counting of cells expressing KI-67-antigen related to total cells (f). Black bars represent 50 µm.

17β-œstradiol weekly, then much below the amounts imposed here (2 mg/kg twice a week). This protocol explains the negative results found for the mice treated by free RU as well as the lack of effective regression by using liposomal formulation. However, despite such unfavourable conditions, antitumoral activity was significantly improved by RU-MFLs and this all the more so the magnetic field gradient was applied to the tumor after each injection. As drug-free MFLs did not act on tumor growing, the positive effect actually arose from the combination of RU with the lipidic carrier which indeed favours its delivery to the estrogen receptor of the MCF-7 cells in a way that RU competed successfully with the particularly high hormone levels jointly administered.

RU is a steroid compound then higly hydrophobic so that it spontaneously and stably fits into the lipid bilayer that constitutes the vesicle shell [33]. Once the liposomes injected to mice, the fate of the drug molecules is then expected to be the same as that of the lipids. Consequently, the long-circulating behaviour of MFLs promoted by their PEG coating is directly transposed to the drug. This led to the antitumor benefit found for mice treated by RU-MFLs compared to free-RU administration, in agreement with previous experiments using non-magnetic nanocarriers [39,40]. In this preclinical study, double *in-vivo* imaging completed by histological analysis and antiproliferative activity asseys newly demonstrated that the injected liposomes effectively reached the tumor as intact objects via the vessels whether in the presence of the magnet or not. On one hand MR imaging and on the other hand fibered confocal microscopy indeed ascertained that the presence of iron oxide in the tumors coincides with the detection of rhodamine fluorescence. This co-localization was yet found in tumoral vessels 18 hours after intravenous administration, totally in accordance with substantive pharmacokinetic data [24]. The immunohistochemical results showed that a part of RU leaves the vascular compartment with the vesicle structures and managed to reach the tumor cells. The efficiency of MFLs to deliver the drug to tumor tissue *via* intravenous route can be easily explained by the rich vascularisation of the xenografts added to passive extravasation due to the leaky endothelial wall characterizing the vessels of such solid tumors [10]. Magnet application obviously boosts this delivery process and induces impressive slow-down of tumor growth. Concomitant co-localization of iron oxide and rhodamine fluorescence in the interstitium added to the significant increase in antiproliferative effect demonstrate that the magnetic field gradient higly concentrates intact RU-loaded MFLs not only in the tumor vessels but actually drives them through the vascular endothelium towards the cancer cells while enhancing drug-cell interaction.

The superparamagnetic maghemite nanocrystals are characterized by high magnetic susceptibility and then maintain large magnetic moments in the presence of external magnetic fields, according to a totally reversible magnetization process. In the presence of a uniform magnetic field gradient as created by an external magnet like that used here, the iron oxide nanoparticles are individually submitted to a force proportional to their magnetization and to the value of the field gradient [41]. When the iron nanoparticles are encapsulated within liposomes, the force by which the liposomes are attracted by the magnet is the sum of all the individual magnetic forces exerted on the grains. As shown in this study, magnetic fluid loading close to 1.5 moles of iron per mole of lipids yielded a global magnetic moment that was sufficient to retain the vesicles in the blood flow with the use of an external magnet producing a gradient of 155 T/m. The magnetic targeting was possible because of the mutual attraction of the magnetized liposomes which indeed behaved as small individual magnets [25]. This synergic process of local accumulation was found interestingly reversible as clearly shown in (Figure 4) where rhodamine fluorescence signals are seen moving along the contour of the blood capillary, indicating that the liposomes were able to circulate again. This suggests that in such magnetic targeting conditions, the risk of thrombosis remains very low.

## Conclusions

This work as a whole demonstrates that magnetic targeting of the pure antiestrogen RU via superparamagnetic liposomes provides an efficient tool for systemic treatment towards breast cancer tumors. The magnetic field gradient, simply produced by a small magnet externally placed onto the tumor, leads to significant accumulation of the in-blood injected liposomes, then of the drug associated to them, within the microvasculature of the malignant tissue. This noticeably increases the probability of extravasation to the perivascular regions of the tumor, facilitating the availability of the drug to the cancer cells. EPR effect is undoubtedly promoted. The steroid antagonist chosen in this study exemplifies the delivery pathway of any other hydrophobic compound which shows affinity for phospholipid bilayers and forms stable mixed vesicle structures. Therefore, beyond the fact that RU-MFLs coupled with magnetic targeting proved here to be promising for the therapy of hormone-dependent breast cancer, this study highlights the potency of the magnetoliposomes themselves. This therapeutic tool indeed allows combination of MRI diagnosis and targeted drug delivery. This deserves to be further investigated in the case of other anticancer agents for the the therapy of breast cancer and/or other

localized cancers. More widely, magnetically modulated nanovesicles provide a unique drug-delivery platform. The preclinical data reported here make possible the use of systemic magnetic targeting to treat solid tumors through the delivery of drugs to the desired target area and fix them at a local site away from the reticuloendothelial system (RES), with the aid of a non-invasive magnetic field. This method should actually improve the therapeutic index of drugs while minimizing side effects.

### Acknowledgements

This work was supported by a grant of the Ministry of Research and the Ligue Nationale contre le Cancer in France. We thank D. Talbot (UMR CNRS 7612, Université Paris 6, France) for iron dosage and V. Nicolas (plateau technique-Imagerie Cellulaire IFR141, Université Paris-Sud 11, France) for technical assistance in confocal microscopy.

### References

1. Jemal A, Siegel R, Ward E, HaoY, Xu J, et al. (2009) Cancer statistics. CA Cancer J Clin **59**:225-249.
2. Cufer T. (2007) Reducing the risk of late recurrence in hormone-responsive breast cancer. Ann Oncol, **18**:8-25.
3. McGuire WL, Chamness GC, Costlow ME, Richert NJ (1975) Steroids and human breast cancer. J Steroid Biochem, 6:723-727.
4. Masamura S, Adlercreutz H, Harvey H, Lipton A, Demers LM, et al. (1995) Aromatase inhibitor development for treatment of breast cancer. Breast Cancer Res Treat 33:19-26.
5. Fisher B, Costantino JP, Wickerham DL, Redmond CK, Kavanah M, et al. (1998) Tamoxifen for prevention of reast cancer: report of the national surgical adjuvant breast and Bowel project P-1 study. J Natl Cancer Inst 90:1371-1388.
6. Jordan VC, Knudson AG (2006) Improvments in tumors targeting, survivorship, and chemoprevention pioneered by tamoxifen. A personal perspective. Oncology (Williston Park) 20:553-562.
7. Hadji P (2009) Aromatase onhibitor-associated bone loss in breast cancer patients is distinct from postmenopausal osteoporosis. Crit Rev Oncol Hematol 69:73-82.
8. Fornander T, Utqvist LE,Wilking N (1991) Effects of tamoxifen on the female genital tract. Ann N Y Acad Sci 622:469-76.
9. Eroles P, Bosch A, Bermejo B, Liuch A (2010) Mechanisms of resistance to hormonal treatment in breast cancer. Clin Trans Oncol 2:246-252.
10. Maeda H (2001) The enhanced permeability and retention (EPR) effect in tumor vasculature: the key role of tumor-selective macromolecular drug targeting. Adv Enzyme Regul 41:189-207.
11. Allen TM, Hansen C, Martin F, Redemann C, Yau-Young A (1991) Liposomes containing synthetic lipid derivatives of poly(ethylene glycol) show prolonged circulation half-lives in vivo. Biochim Biophys Acta 1066:29-36.
12. Immordino ML, Dosio F, Cattel L (2006) Stealth liposomes: review of the basic science, rationale, and clinical applications, existing and potential. Int J Nanomedicine 1:297-315.
13. Salzberg M, Thurlimann B, Hasler U, Delmore G, von Rohr A, et al. (2007) Pegylated liposomal doxorubicin (caelyx) in metastatic breast cancer: a community-based observation study. Oncology 72:147-151.
14. Andresen TL, Jensen SS, Jorgensen K (2005) Advanced strategies in liposomal cancer therapy: problems and prospects of active and tumor specific drug release. Prog Lipid Res 44:68-97.
15. Song S, Liu D, Peng J, Sun Y, Li Z, et al. (2008) Peptide ligand-mediated liposome distribution and targeting to EGFR expressing tumor in vivo. Int J Pharm 363:155-161.
16. Hafeli UO (2004) Magnetically modulated therapeutic systems. Int J Pharm 277:19-24.
17. Shinkai M, Ito A (2004) Functional magnetic particles for medical application. Adv Biochem Eng Biotechnol 91:191-220.
18. Alexiou C, Schmid RJ, Jurgons R, Kremer M, Wanner G, et al. (2006) Targeting cancer cells: magnetic nanoparticles as drug carriers. Eur Biophys J 35:446-450.
19. Nobuto C, Sugita T, Kubo T, Shimose S, Yasungaga Y, et al. (2007) Evaluation of systemic chemotherapy with magnetic liposomal doxorubicin and a dipole external electromagnet. Int J Cancer 109:627-635.
20. Martina MS, Fortin JP, Ménager C, Clément O, Barratt G, et al. (2005) Generation of superparamgnetic liposomes revealed as highly efficient MRI contrast agents for in vivo imaging. J Am Chem Soc 127:10676-10685.
21. Fortin-Ripoche JP, Martina MS, Gazeau F, Ménager C, Wilhelm C, et al. (2006). Magnetic targeting of magnetoliposomes to solid tumors with MR imaging monitoring in mice: feasibility. Radiology 239:415-424.
22. Martina MS, Fortin JP, Fournier L, Ménager C, Gazeau F, et al. (2007) Magnetic targeting of rhodamine-labeled superparamagnetic liposomes to solid tumors : in vivo tracking by fibered confocal fluorscence microscopy. Mol. Imaging 6:140-146.
23. Martina MS, Nicolas V, Wilhelm C, Ménager C, Barratt G, et al. (2007) The in vitro kinetics of the interactions between PEG-ylated magnetic-fluid-loaded liposomes and macrophages. Biomaterials 28:4143-4153.
24. Plassat V, Martina MS, Barratt G, Ménager C, Lesieur S (2007) Sterically stabilized superparamagnetic liposomes for MR imaging and cancer therapy : pharmacokinetics and biodistribution. Int J Pharm 344:118-127.
25. Riviere C, Martina MS, Tomita Y, Wilhelm C, Tran Dinh A, et al. (2007) Magnetic targeting of nanometric magnetic-fluid-loaded liposomes to specific brain intravascular areas : a dynamic imaging study in mice. Radiology 244:439-448.
26. Martina MS, Wilhelm C, Lesieur S (2008) The effect of magnetic targeting on the uptake of magnetic-fluid-loaded liposomes by human prostatic adenocarcinoma cells. Biomaterials 29(30):4137-4145.
27. Marsaud V, Gougelet A, Maillard S, Renoir JM (2003) Various phosphorylation pathways, depending on agonist and antagonist binding to endogenous estrogen receptor alpha (ERalpha), differentially affect ERalpha extractability, proteasome-mediated stability, and transcriptional activity in human breast cancer cells. Mol Endocrinol 17:2013-2027.
28. Galman MS, Sundstrom, SA, Little, CR (1990) Antagonism of estrogen- and antiestrigen-induced uterine complement component C3 expression by ICI 164,384 J Steroid Biochem 36: 281-286.
29. Wakeling AE, Dukes M, Bowler J (1991) A potent specific pure antiestrogen with clinical potential. Cancer Res 51:3867-3873.
30. Van de Velde P, Nique F, Bouchoux F, Brémaud J, Hameau MC, et al. (1994) RU 58668 A new pure antiestrogen inducing a regression of human mammary carcinoma implanted in nude mice. J Steroid Biochem Mol Biol 48:187-96.
31. Van de Velde P, Nique F, Brémaud J, Hameau MC, Philibert D, et al. (1995) Exploration of the therapeutic potential of the antiestrogen RU 58668 in breast cancer treatment. Ann N Y Acad Sci 761:164-175.
32. Van de Velde P, Nique F, Planchon P, Prévost G, Brémaud J (1996) RU 58668: further in vitro and in vivo pharmacological data related to its antitumoral activity. J Steroid Biochem Mol Biol 59:449-457.
33. Plassat V, Wilhelm C, Marsaud V, Ménager C, Gazeau F (2011) Magnetic targeting of superparamagnetic liposomes loaded with the antiestrogen RU 58668 provides a highly efficient tool for selective activity against human breast cancer cells. Adv Funct Mat 21: 83-92.
34. Massart R (1982) Preparation of aqueous magnetic liquids in alkaline and acidic media. US Patent 4329241.
35. Lesieur S, Grabielle-Madelmont C, Ménager C, Cabuil V, Dahdi D, et al. (2003) Evidence of surfactant-induced formation of transient pores in lipid bilayers by using magnetic-fluid-loaded liposomes. J Am Chem Soc 125:5266-5267.
36. Ameller T, Marsaud V, Legrand P, Gref R, Renoir JM (2003) In vivo and in vitro biological evaluation of biodegradable long circulating carriers loaded with the antiestrogen RU 58668. Int J Cancer 106:446-454.

**Citation:** Plassat V, Renoir JM, Autret G, Marsaud V, Ménager C, et al. (2013) Systemic Magnetic Targeting of Pure-Antiestrogen-Loaded Superparamagnetic Nanovesicles for Effective Therapy of Hormone-Dependent Breast Cancers. J Bioanal Biomed 5: 028-035. doi:10.4172/1948-593X.1000077

37. Lippman M, Bolan G, Huff K (1976) The effects of estrogens and antiestrogens on hormone-responsive human breast cancer in long-term tissue culture. Cancer Res 36:4595-4601.

38. Steel CD, Stephens AL,Singletary SJ, Ciavarra RP (2008) Comparison of the lateral tail vein and the retro-orbital venous sinus as routes of intravenous drug delivery in a transgenic mouse model. Lab Anim (NY) 37:26-32.

39. Renoir JM, Stella B, Amellier T, Connault E, Opolon P, et al. (2006) Improved antitumoral capacity of mixed and pure antiestrogens in breast cancer cell xenografts after their administration by entrapment in colloidal nanosystems. J Steroid Biochem Mol Biol 102:114-27.

40. Maillard S, Ameller T, Gauduchon J, Gouilleux F, Legrand P, et al. (2005) Innovative drug delivery nanosystems improve the antitumor activity in vitro and in vivo of antiestrogens in human breast cancer and multiple myeloma. J Steroid Biochem Mol Biol 94:111-21.

41. Wilhelm C, Gazeau F, Bacri JC (2002) Magnetophoresis and ferromagnetic resonance of magnetically labeled cells. Eur Biophys J 31:118-25.

This article was originally published in a special issue, **Liposome Drug Delivery** handled by Editor(s). Dr. Wong Jonathan, University of Edinburgh, Canada